

FERMILAB-Proposal-0653 Spokesperson: Neville W. Reay
Department of Physics
Ohio State University
Columbus, Ohio 43210
614-422-7436
FTS (8) 940-7436

A PROPOSAL TO MEASURE CHARM AND R DECAYS
VIA HADRONIC PRODUCTION IN A
HYBRID EMULSION SPECTROMETER

N. Ushida
Aichi University of Education, Kariya, Japan

M. Johnson
Fermi National Accelerator Laboratory, Batavia, Illinois

G. Fujioka, H. Fukushima, C. Yokoyama
Physics Department, Kobe University, Kobe, Japan

Y. Homma, Y. Tsuzuki
Faculty of Liberal Arts, Kobe University, Kobe, Japan

S. Y. Bahk, C. O. Kim, J. N. Park, J. S. Song
Korea University, Seoul, Korea

H. Fuchi, K. Hoshino, K. Niu, K. Niwa, H. Shibuya, Y. Yanagisawa
Department of Physics, Nagoya University, Nagoya, Japan

J. Kalen, S. Kuramata, N. W. Reay,
K. Reibel, R. A. Sidwell, N. R. Stanton
Department of Physics, Ohio State University, Columbus, Ohio

K. Moriyama, H. Shibata
Faculty of Sciences, Okayama University, Okayama, Japan

T. Hara, O. Kusumoto, Y. Noguchi, M. Teranaka
Osaka City University, Osaka, Japan

J.-Y. Harnois, C. D. J. Hebert, J. Hebert, B. McLeod
Department of Physics, University of Ottawa, Ottawa, Ontario, Canada

H. Okabe, J. Yokota
Science Education Institute of Osaka Prefecture, Osaka, Japan

S. Tasaka
Institute for Cosmic Ray Research, University of Tokyo, Tanashi, Tokyo, Japan

T. S. Yoon
Department of Physics, University of Toronto, Toronto, Ontario, Canada

R. Heisterberg
Department of Physics, Virginia Tech, Blacksburg, Virginia

J. Kimura, Y. Maeda
Yokohama National University, Yokohama, Japan

May 1, 1980

4485114

Table of Contents

	<u>Page</u>
A. Summary of Experiment	3
B. Physics Motivation	3
C. Description of Experiment	5
1. Design Motivation	5
2. Solid State Detectors	7
3. Discussion of Apparatus	8
a. Beam	8
b. Emulsion	9
c. Vertex Detector	10
d. Charged Particle Spectrometer	12
e. Gamma Detector	14
f. Calorimeter	15
g. Muon Detector	16
h. Trigger Counters	17
D. Experimental Rates and Acceptances	18
E. Cost Estimates	22
F. Time Scale for Experiment	25
References	27
Figures	
1. Captions	28
2. Figures 1 - 10	30
Appendices	
I Prototyping Solid State Detector	40
II Event Reconstruction	44

A. Summary of the Experiment

We propose an experiment which employs a hybrid emulsion spectrometer to measure lifetimes and decay properties for B mesons and charmed particles produced by interactions of high energy pions. Use of a high-momentum pion beam should maximize the B production cross-section at presently available energies; emulsion is the highest resolution detector for observing short lifetimes, and the electronic detection system is needed to select interesting events, locate them within the emulsion and provide information about decay products. A variation of this technique has proven successful in measuring the lifetimes of neutrino-produced charmed particles (Fermilab Experiment 531). We believe that the experience therein gained will permit us to switch to hadronic production, where there are more B and charmed particles to be found, and also more problems. Subject to development of a new form of solid-state detector, in a four month run with modest beam we should be able to obtain more than 1000 charmed particle decays, and based on a 100 nb cross-section, about 30 B decays. There is also hope of seeing a small number of tau-lepton decays.

Developing the new detector will require one to two years, thus actual running of the experiment could not take place before 1983. Though yields in the proposal are quoted for 400 GeV operation, based on the threshold behavior for ψ production we estimate that the signal for B production would be improved a factor of four if the experiment were run at Tevatron energies.

B. Physics Motivation

We wish simultaneously to search for B-meson decays and to make a high statistics measurement of charm decays.

The latter measurement provides an acceptable and secure motivation for the experiment. A $\pm 10\%$ knowledge of lifetimes permits conversion of

branching ratios into absolute partial decay rates without loss of precision. A current experiment¹ shows hints of two neutral lifetimes and possibly the existence of weakly decaying neutral charmed baryons. Definitive studies of the above plus the possibility of observing sequential $F \rightarrow \tau \rightarrow \text{other}$ lepton decays creates interest in a high statistics charm measurement. Observation of visible decay lengths also provides a relatively background-free sample of charmed particles for studying production dynamics. Provided trigger rates are acceptable, we may request a second run with geometry expanded to include particle identification.

However, the discovery of the upsilon family of resonances, and particularly the broad γ''' , is considered to be strong evidence for the existence of b quarks, hence B mesons and baryons.

This experiment will have three nanobarn sensitivity for detecting B mesons, provided lifetimes are between 3×10^{-15} and 3×10^{-12} seconds. Should B mesons exist at this level, their sequential $B \rightarrow \text{charm} \rightarrow \text{strange}$ decays should be topologically quite striking and relatively background free. In terms of the Kobayashi-Maskawa² six quark model, measurement of the B meson lifetimes and relative branching ratios into charm would permit determination of the extended Cabibbo angles θ_2 and θ_3 (where θ_1 is the usual Cabibbo angle θ_c). As all angles and CP violating phases are expected to be small, we can approximate

$$\begin{aligned} \sin \theta_i &\equiv s_i \\ \cos \theta_1 &= \cos \theta_2 = \cos \theta_3 = 1 \end{aligned}$$

If we also assume the ratio,

$$\frac{(B \rightarrow \text{charm} + X)}{(B \rightarrow \text{no charm})} \approx \left| \frac{s_3 + s_2 e^{i\delta}}{s_1 s_3} \right|^2 \gg 1$$

Then,

$$\tau_B \approx \left(\frac{M_C}{M_B} \right)^5 \frac{1}{|s_3 + s_2 e^{i\delta}|^2} \tau_{\text{charm}}$$

The θ_i are given in terms of quark mass ratios by many of the higher symmetry models which predict proton decay,³ and charm lifetimes are 10^{-13} to 10^{-12} seconds;¹

$$\tau_B \approx \left(\frac{1.9 \text{ GeV}}{5.3 \text{ GeV}} \right)^5 (10 - 100) (10^{-13} \text{ to } 10^{-12} \text{ seconds})$$

$$\tau_B \approx 5 \times 10^{-15} \text{ to } 5 \times 10^{-13} \text{ seconds}$$

Should B lifetimes lie in this measurable range, the Higgs particle would have to be heavier than the B, else τ_B would be considerably shorter.

However, it may be that the b quark (and perhaps the tau lepton) are not members of doublets. In this case, theoretical predictions have even more freedom, and information obtained on B-meson decays could prove to be even more exciting.

C. Description of the Experiment

1. Design Motivation

The apparatus is a hybrid emulsion spectrometer similar in concept but technically more demanding than the one used successfully in experiment 531, and it will be operated in a π^- beam rather than in a neutrino beam. The sensitivity of the experiment is ultimately limited by the volume of emulsion (50ℓ) and the maximum tolerable track density ($700/\text{mm}^2$) to a total of 7×10^7 interactions. It is feasible to search for $1 - 2 \times 10^4$ of these events in the emulsion, so it is important a) to find efficient selection criteria and b) to eliminate unnecessary losses of good events due to spectrometer acceptance and reconstruction and scanning inefficiencies.

The configuration and mounting of the emulsion is determined by the following considerations: 1) The thickness along the beam direction should be as small as possible to reduce secondary interactions, but not so small

that edge effect losses are serious. 2) The exposure area (beam spot size) must be large enough so that the maximum exposure density does not occur in less than one beam pulse, since moving the emulsion more often than this is not practical. 3) Unnecessary exposure of emulsion outside the beam due to beam halo should be minimized. 4) Precise alignment of emulsion relative to the spectrometer must be performed. These considerations lead to a design in which many small modules $\sim (10\text{cm})^2 \times (2 - 3\text{cm thick})$ are sequentially exposed at the rate of one every 1 - 2 hours. Each small module is mounted on a precision movable stage which allows exposure of a different $(7\text{mm})^2$ area to every beam pulse.

The design of the electronic spectrometer is motivated by the following requirements: 1) Finding events in the emulsion quickly and efficiently-- This is probably best done by following a tagged beam track. Since the average separation of beam tracks in the emulsion will be only $\sim 40\mu$. unambiguous tagging requires position resolutions $\sim \pm 20 \mu$. 2) Large acceptance for beauty (B) and charm (C) decay products; 3) Good reconstruction efficiency for high-multiplicity, sharply-collimated events typical of hadronic interactions at 375 GeV; 4) Minimum decay path for π 's and K's-- Since we will depend on a single- μ trigger, the apparatus must be kept short. 5) Ability to detect secondary vertices-- The relatively long lifetime of the $D^\pm (10.3^{+10.5}_{-4.1} \times 10^{-13} \text{ sec})^1$ makes feasible the efficient selection of a highly enriched D^\pm sample (and some D^0 , F^\pm , and Λ_c as well) by successfully resolving production and decay vertices with the electronic spectrometer. Excellent position resolution in the detector downstream of the emulsion therefore becomes very desirable. 6) Successful kinematic reconstruction of B and C events, implying satisfactory momentum resolution for charged particles and the ability to detect neutrals.

2. Solid State Detectors

It is very difficult to satisfy the above design criteria with existing technology. Drift chambers, for example, fall short of the position resolution required for beam tagging and decay vertex resolution by factors of ~ 7 . Even worse, they can achieve track pair resolution no better than about 2mm, so that tracks more closely spaced than this are lost. Since projected angles between tracks of ≤ 1 mrad occur with appreciable probability in hadron interactions at 375 GeV, it is impossible to place drift chambers close to the emulsion target without incurring unacceptable reconstruction losses. (Yet, high resolution detectors close to the emulsion target are essential if the apparatus is to be kept short.)

We have therefore produced a spectrometer design which relies heavily on a new technology, that of position-sensitive silicon detectors⁴, and have begun a program of prototyping and testing. More details are provided in Appendix I. Briefly, these proposed devices are thin silicon semiconductor detectors on which are deposited many narrow parallel metal strips with a center-to-center spacing of 40μ (Figure 1). These strips are to be read out individually over a limited area corresponding to the region of highest track density, and will be read out in groups using the charge-interpolation technique⁵ with taps every 5 to 10 strips in regions where the average track density is lower. In designing the spectrometer we have assumed that we will succeed in producing detectors with the following characteristics: (1) active area up to 8cm diameter; (2) thickness 0.4mm; (3) position resolution $\pm 20\mu$; (4) track pair resolution 40μ ; (5) successful operation in magnetic fields ≤ 1.0 T. There is at present no reason to believe that any of these requirements are unreasonable.

3. Discussion of Apparatus

A schematic elevation view of the experiment is shown in Figure 2. Note that the total length of the apparatus between the emulsion target and the upstream side of the calorimeter is less than 1.5m. The major components are the beam and beam detectors, emulsion target, vertex detector, charged particle spectrometer, γ detector, neutral hadron detector, muon identifier, and trigger counters.

a. Beam and beam detectors. Because of the expected rapid increase of B cross section with energy, a π^- beam of the highest available momentum (~375 GeV) is essential. The momentum bite can be large, and an intensity $\sim 2 \times 10^4$ /pulse is satisfactory. The optimum spot size at the emulsion is 0.7cm square. Because the emulsion target is much larger than this and will be shifted by one spot size after each beam pulse, it is very important that the integrated halo for several centimeters around the beam is a small fraction of the total intensity to avoid increasing the level of background tracks in the emulsion.

To keep the emulsion exposure density uniform, a beam plug with an out-to-in response time of 0.1 second which can be actuated by a preset beam counter must be incorporated well upstream in the beam line.

The transverse coordinates of beam tracks at the emulsion will be determined to $\pm 20\mu$ by three small silicon detectors (called SS triplet in Figure 2) of the type shown in Figure 1-a, located immediately upstream of the emulsion. It is also desirable to determine beam track slopes to better than ± 0.02 mrad for use in surveying the rest of the apparatus. A second set of three silicon detectors is therefore located 2.0m further upstream.

b. Emulsion. Nuclear emulsion is a suitable detector to observe short-lived particles with lifetime of 3×10^{-15} to 3×10^{-12} seconds. One can handle enough emulsion to get relatively rare events, but the limitation of using it is in analyzing large numbers of events under the microscope.

Recently a microscope with TV monitor and computer-controlled, digitized stage has been developed at Nagoya University and has turned out to be very powerful in analyzing E531 neutrino events.

In this experiment we will use as much emulsion as possible and as high a track density as tolerable to get good sensitivity to small cross sections. The total amount of emulsion we can handle is about 50%, and is limited primarily by cost. Maximum tolerable intensity is a slightly subjective number but is around $(6 \pm 2) \times 10^4 / \text{cm}^2$. We can get more than 7×10^7 interactions using 50% of emulsion and 2×10^4 /pulse beam intensity. To reduce the secondary phenomena, e.g., γ -ray conversion and secondary interactions, the thinner the emulsion module along the beam direction the better. But we have to reduce edge effects especially for the pellicles. The compromised depth is 2 - 3cm. The track density at the downstream end of modules is then 1.5 times as much as at the upstream end. We can get some information about maximum tolerable intensity from NA-19 at CERN, in which Nagoya people are involved.

Although the area of each emulsion module is about 10cm x 10cm, the size of beam spot is around 7mm x 7mm, and therefore we must have some movable stage to expose uniformly over the whole area.

The accuracy of track detectors is so high that we have to be careful in mounting the emulsion module. A schematic drawing of the stage is shown in Figure 3. It is driven by computer-controlled pulse motors and the position of the stage is monitored by moiré image encoders (1 μ m accuracy) or

by laser diffraction encoders ($0.1\mu\text{m}$ accuracy). In this way we can know the relative position of events in the module. We also need to know the relative position of the module and the counter systems with an accuracy of $10\mu\text{m}$. For this purpose we will expose two low-beam density regions ($1\text{cm} \times 1\text{cm}$). The total number of tracks in each of these regions will be about 100. Since beam tracks may easily be found in these low-density regions, translations transverse to and rotations about the beam line may be removed on a module by module basis. This will permit much greater precision for event searches in regions of high track density.

The events located by the spectrometer will be found by two methods. One is to follow the incident beam; another is conventional volume scanning. We will tag the incident beam which produced interesting events. We can follow all the tracks seen in one field of view. In this case we do not need very good accuracy. If the vertex predictions are sufficiently good, we can also use the conventional volume scan technique. The volume is estimated to be about 0.1mm^3 , which is about two orders of magnitude smaller than in E531, implying that the event finding speed is 100 times faster than before, exclusive of set-up time.

After events are found, each will be analyzed using a microscope with a simplified computer-guided, digitized stage. In this fashion we can fully analyze 5000 events a year, and inspect several times this many.

c. Vertex detector. The vertex detector consists of 15 silicon detectors arranged in 5 triplets mounted on 2.5cm centers. Each triplet measures 3 projections rotated 60° from each other (x,u,v). With the proposed $\pm 20\mu$ resolution the direction of stiff tracks can be measured to $\pm 0.2\text{mrad}$ in each projection. Each detector (Figure 1-b) has an active area of 8cm diameter and is only 0.4mm thick to reduce multiple scattering. In the

central 1.4cm band of each detector every strip is read out separately to maintain 40μ track-pair resolution in the region of high track density. On either side of this central band the charge interpolation technique is used, with pulse height information from taps every 5 to 10 strips being read out, thus preserving the spatial resolution but relaxing the track-pair resolution.

We have studied the track-pair resolution requirements by use of a tape of measured 360 GeV π^-p events from a 30" bubble-chamber exposure. The real tracks were augmented by gammas from Monte Carlo π^0 's which were allowed to convert with appropriate probability in a simulated 3cm emulsion target.

The results of this study are summarized in Figure 4 and Table 1.

Table 1. Chamber parameters

Location	Z (cm)	Approx. θ (mrad)	Track pair resolution (microns)	Track pair resolution $\Delta x'$ (mrad)	Fraction of tracks blocked
Center of vertex detectors	~10	0 - 50	40μ	0.4	<9%
		50 - 150	200μ	2.0	<8%
		>150	400μ	4.0	<8%
Downstream silicon detectors	~80	0 - 50	400μ	0.50	<10%
Downstream drift chambers	~80	>50	2000μ	2.5mrad	<10%

The integral distribution in laboratory production angle θ for all charged tracks in this sample is shown in Figure 4-a. Approximately half the tracks have $\theta < 50\text{mrad}$ and 25% have $\theta < 12\text{mrad}$. Since the mean multiplicity of

charged hadrons and converted electrons is ~ 14 , the effects of track masking can be appreciable. In Figure 4-b we plot the fraction of tracks produced at θ which are masked in a given projection (x, e.g.) for various assumed slope resolutions $\Delta x'$. If, for example, the detector can resolve two tracks if their projected slopes differ by more than 0.4 mrad, the fraction of masked tracks is $< 9\%$ at all θ . This condition obtains in the middle of the vertex detector ($z = 10\text{cm}$) where the pair resolution Δx is 40μ , giving $\Delta x' = 0.4\text{mrad}$. For $\theta > 50\text{mrad}$ ($> 150\text{mrad}$) a $\Delta x'$ of 2.0mrad (4.0mrad) is sufficient to keep the masking below 10%. The outer regions of the silicon detectors therefore use the charge interpolation method. Similar considerations are used in designing the detectors downstream of the magnet (next section).

It should be noted that because the silicon detectors are thin it will be necessary to operate them at low temperature (-100°C) to obtain satisfactory signal/noise. The whole vertex detector must therefore be cryogenic.

The signal from each tap, or from each strip in the central region of the vertex detector, will require a low-noise amplifier and analogue readout. There are a total of 13,000 such lines in the beam, vertex and spectrometer arrays of silicon devices. We plan to store the analogue information in charge-coupled devices (CCD's) and digitize this data serially during readout.

d. Charged particle spectrometer. In order to achieve maximum aperture and minimum depth we have designed the spectrometer around the small iron magnet shown in Figures 1' (layout), and 5 (B-field).

This magnet has a pole-piece depth of only 35cm and allows a vertical aperture from the target of $\pm 240\text{mrad}$ with a maximum vertical gap of 26cm.

The horizontal aperture is twice as large. By having the pole pieces open vertically outward (thereby deliberately creating a non-uniform field) a transverse kick of 0.20 GeV/c is obtained with a maximum field of 2.1T.⁶

The directions of charged particles downstream of the magnet are measured by silicon detectors at small angles and by drift chambers similar to those used in E531 at larger angles. The silicon detectors are of the type shown in Figure 1-c, with active areas of 8cm diameter and charge-interpolation readout with taps every 10 strips. There are 3 pairs of xuv triplets located at approximately 75, 85 and 110cm from the target. Stiff tracks with production angles $\theta \leq 50\text{mr}$ pass through the first two pairs, while those with $\theta \leq 40\text{mrad}$ pass through all three. If we use the rule of thumb that most B-meson and charm-decay tracks have $p_T \leq 1 \text{ GeV}/c$, these silicon detectors measure momenta of most tracks having $p \geq 20 \text{ GeV}$. For tracks with $\theta \geq 50\text{mr}$, which are on the average softer and more widely separated, a system of 12 drift chambers (4 pairs of xuv triplets) measure the directions with spatial resolution $\pm 150\mu$ and a lever arm of 30cm. As can be seen from the momentum resolution graphs in Figure 6, with this multi-element system momenta $p \leq 3 \text{ GeV}/c$ are measured to $\pm 1.5\%$, while most tracks at 50 GeV/c are still measured to $\pm 6\%$.

It is clear that to use the excellent resolution of silicon detectors to full advantage we must build stable mounting hardware and monitor the alignment carefully. Our experience with the much larger apparatus in E531 should be most useful here. In that experiment drift-chamber positions were found to be stable to $\pm 25\mu$ over times ~ 1 week, and absolute survey discrepancies between the drift chambers and emulsion fiducial sheet were $\sim \pm 50\mu$. In addition, we can record stiff beam tracks passing through the central regions of all the high-resolution devices, a very powerful survey tool which we did not have in E531.

e. Gamma detector. For electron/photon detection we have designed a segmented electromagnetic shower calorimeter consisting of alternate layers of 1 radiation length of lead and extruded aluminum proportional ionization chambers (EPIC). A similar device has been tested satisfactorily for use in E531. The overall dimensions of the detector are 1m x 1m with a total thickness of 14 radiation lengths of lead. Each EPIC chamber is constructed of aluminum extrusions with individual tube cross sections of 1cm x 1cm. The pulse heights from each tube will be read out from both ends using a charge-division technique to give both x and y position information from each chamber. The spatial resolution attainable with this technique is typically 1% of the wire length or ~1cm along the direction of the wire for a 1m chamber. To reduce the number of ADC channels required the pulse heights from groups of 32 tubes will be stored in a parallel input CCD and serially shifted into an ADC for digitization.

With one radiation length of lead sampling thickness, similar devices⁷ using multi-wire proportional chambers operated at 1 atmosphere of pressure have achieved an energy resolution $\Delta E/E = 0.30/\sqrt{E}$. This is about a factor of two worse than the resolution obtained with a lead-scintillator calorimeter. We expect to operate the gamma EPIC chambers at a pressure of ~10 atmospheres and estimate an improved energy resolution of $0.20/\sqrt{E}$.

Assuming a spatial resolution of ~2.0cm for showers, Monte Carlo studies using 350 GeV π^-p events from a 30" bubble chamber exposure indicate an overall efficiency of ~70% for resolving multiple showers in the γ -detector. Masking of one shower by another is worst in the central core for angles less than 50mrad. Here the efficiency drops to ~40%. We are investigating the feasibility of using silicon detectors with lead converters to cover this central 50mrad with better position resolution.

Additional details and discussion of the spatial and energy resolution can be found in Appendix II.

f. Hadron calorimeter. The primary function of the hadron calorimeter is to measure the position and energy of neutral hadrons (K^0 , Λ^0 , and n). The position resolution that can be achieved is $\leq 25\text{mm}$, or $\sim 20\text{mrad}$ at 1.3m .⁸ This angular resolution is well matched (in terms of contributions to the overall mass resolution) by an energy resolution of $\sim 1/\sqrt{E}$ for the range of energies of interest (5-25 GeV).

The major difficulty in finding neutral hadrons lies in separating them from the charged hadron background. We have estimated the detection efficiency by plotting the positions of charged hadrons at the front face of the calorimeter. A successful identification is assumed if no other hits lie within $\pm 40\text{mrad}$ ($\pm 5\text{cm}$) in the x projection. The resulting efficiency is shown in Figure 7 as a function of polar angle θ . Superimposed on this curve is the kaon angular distribution expected from $B \rightarrow \psi K^0 \pi$. The net efficiency, including corrections due to loss of events with $p_{K^0} < 5\text{ GeV}$, and a finite absorber thickness ($1 - e^{-2} \approx .84$) is 25%.

The proposed detector is shown in Figure 2. It consists of alternate layers of iron plates and extruded MWPC (EPIC chambers) with 2.54cm wire spacing operated at atmospheric pressure. We are using EPIC chambers of this kind in the second run of E531 and have tested sample chambers in the M5 beam line. The iron plates, which can be made from the E531 calorimeter steel with a minimum of cutting, have dimensions 1.2m high x 1.5m wide x 5cm thick for the first six plates, 2.4m x 3.0m x 10cm for the next two, and 2.4m x 3.0m x 20cm for the last 3 plates. EPIC chambers covering $\pm 240\text{ mrad}$ from the target are inserted after each of the plates, and are read out from both ends using the charge division technique to give coupled two-dimensional information on the hit positions as is done in the gamma

detector. A total of 1,728 amplifiers is required. The analogue data will be stored in CCD's and digitized serially during readout.

g. Muon detector. The muon detector has two functions: to reduce the hadron flux sufficiently to give a manageable trigger rate, and to determine from the reconstructed event whether a given track which has traversed the detector is indeed a muon. The first objective is most simply accomplished by requiring enough range of iron. Using simulated decays of measured tracks from a 360 GeV bubble chamber exposure we found that 2.5m of iron (including that in the calorimeter) will give fewer than 20 triggers/10³ interactions from upstream decays and punch through, while accepting muons above 3.5 GeV/c.

To meet the second objective it is essential to track the muon candidate from the emulsion through the spectrometer, hadron calorimeter, and absorber with frequent sampling of position and ionization in the iron to look for evidence of hadronic interaction. It is also very desirable to make a second momentum measurement after several interaction lengths of iron to be sure that no large energy loss has occurred, and that the correct candidate has been tracked through the region of heavy hadron showers.

The frequent sampling is performed in the EPIC chambers of the calorimeter. The second momentum measurement is performed with a square iron toroid (similar to those used in E613) 1.0m deep and 2.5m on a side. Assuming low carbon steel (1010 or equivalent), a current of 1000 Amp and 100 turns, one obtains reasonable saturation and a radial variation of magnetic field from 2.0 T near the center to 1.7 T at the outer rim. On either side of this toroid are 2 triplets of EPIC chambers instrumented for drift-chamber readout using surplus electronics from E531. This system will have a resolution

$$\frac{\delta p}{p} = \left[(.21)^2 + (.01p)^2 \right]^{\frac{1}{2}}, \quad (p \text{ in GeV/c})$$

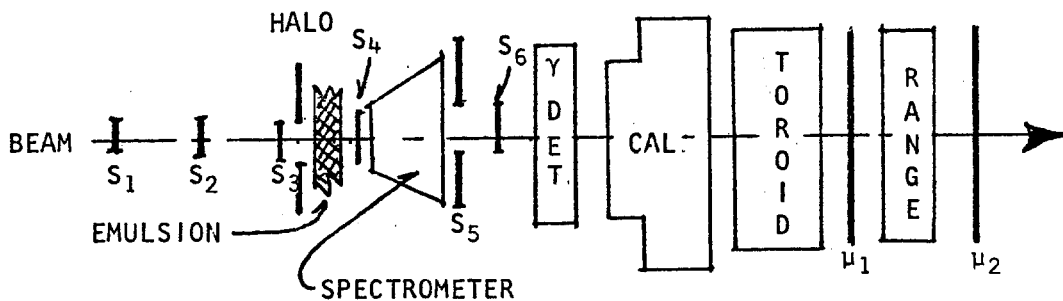
where the first term is the multiple scattering contribution and the second results from the $\pm 0.5\text{mm}$ resolution of the chambers.

Downstream of the toroid are three identical modules, each consisting of 0.4m of steel followed by two crossed bands of EPIC chambers with 5cm wire spacing, with each tube read out from both ends to give charge-division information. The final two modules serve to further constrain muon candidates above 3.5 GeV/c.

h. Trigger counters. As non-zero data from all events will be stored in a fast buffer memory during each spill, we are studying a variety of triggers, many of which require fast processing before recording on magnetic tape.

Though several techniques appear promising, we will present here only the simplest muon trigger, which should be sufficient to lower recorded events to a level of 20/pulse. This trigger will require non-halo beam to interact in the emulsion, giving rise to a downstream muon of more than 3.5 GeV.

The following sketch qualitatively indicates counter locations:



The trigger will consist of

$$\text{Trigger} = (\text{Beam}) \cdot (\text{Interaction}) \cdot (\text{Muon})$$

with components as listed below:

$$\text{Beam} = S_1 \cdot S_2 \cdot S_3 \cdot \overline{\text{Halo}}$$

$$\text{Interaction} = (S_4 \geq 4 \text{ in pulse height}) \cdot (S_5 \geq 2 \text{ pulse height})$$

(S_5 will have a small hole for non-interacting beam)

$$(\text{Muon}) = \mu_1 \cdot \mu_2$$

(The muon counters may have to be shielded against slow neutrons.)

D. Event Rates and Acceptances

In the standard model the B meson is expected to have a substantial branching ratio (B.R.) to muons either from direct decay:

$$(a) B \rightarrow \mu + \text{anything}$$

or through the cascade

$$(b) B \rightarrow D + \text{anything}$$

$$\quad \quad \quad \downarrow$$

$$\quad \quad \quad \mu + \text{anything}$$

In the first case, the muons are stiff and have a large transverse momentum ($p_T \sim 1 \text{ GeV}/c$), while in the second case they are soft and have $p_T \sim 0.3 - 0.4$. We have therefore considered two methods of analysis of events; the first a tag of B decays with a stiff muon, the second a tag of events passing less stringent cuts on the muon, but having a reconstructed secondary vertex. The second analysis will also yield a large sample of charm decays.

Tagging interesting decays with muons requires that we can extract a signal out of the background of soft muons coming from π decays upstream of (as well as in) the calorimeter. We have generated muon spectra from pion decays (using 360 GeV/c π^- bubble-chamber data) and from $B \rightarrow \mu$ via Monte Carlo simulation of processes (a) and (b) above. The decay distance allowed is 120cm. We assume the B's are centrally produced with

$$\frac{d\sigma}{dx dp_{\perp}} = c(1-x)^N e^{-ap_{\perp}}$$

In figures 8 and 9 we compare the p and p_T distributions for muons from these three sources, where we have taken $N = 2$ and $a = 1$ in the expression above in generating the B mesons. We have also calculated the muon spectrum for the process $K \rightarrow \mu\nu$ (not shown). The muon background is listed in Table II for several values of p and p_T .

Table II, Muon background per 360 GeV/c π^- interaction.

Off-line selection	P_μ GeV/c	P_T GeV/c	$\pi \rightarrow \mu$	$K \rightarrow \mu$
a	> 6	> 0.6	3×10^{-4}	0.5×10^{-4} (+ secondary vertex)
b	> 3.5	> 0.25	4×10^{-3}	4×10^{-4}

We have assumed $1/3$ K^\pm /interactions, and a 63% B.R. to $\mu\nu$.

In addition to the decays of primary pions and kaons, one also has muons produced by decays of secondary and tertiary pions produced in the hadron absorber. This latter background is comparable to that listed in Table I but can largely be eliminated by comparing momenta of muons as measured in the spectrometer and in the toroid and by requiring that the muon point to the interaction vertex.

The yield of events is given by

$$\text{Yield} = (\text{No. interactions}) \times (\text{electronic live time}) \times (\text{scanning efficiency}) \\ \times \left(\frac{\sigma_B}{\sigma_{\text{abs}}} \right) \times \text{B.R.} \left(\frac{B \rightarrow \mu}{B \rightarrow \text{all}} \right) \times (\mu \text{ detection efficiency}).$$

A similar expression may be used for the charm yield.

We take the number of interactions to be 7×10^7 , the electronic live time to be 80%, and the scanning efficiency to be 50% (the efficiency in E531 is 53%). $\sigma_{\text{abs}} = 8.7 \text{mb/nucleon}$ for pions in emulsion.

We calculate B yields based on a total cross section of 100 nb/nucleon.

This estimate is motivated in part by Figure 10 where we compare the πp inclusive cross sections for the bound quark states ϕ , ψ , T to the unbound states K , charm.⁹ The bound states differ in cross section by 8 decades, yet they lie on a straight line. If we assume that the unbound states also lie on a straight line with a slope determined by the K and charm cross sections, we get a B cross section of approximately 200 nb/nucleon. Published theoretical estimates range from 8nb to $\sim 1\mu\text{b}$.¹⁰ The Goliath result from CERN, if correct, would imply a cross section of several hundred nanobarns.

In the free quark model the b quark decays directly to muons (plus hadrons) with a B.R. $\approx 16\%$. Non-leptonic enhancements will reduce this ratio, especially for the B^+ which decays non-exotically, so we take the average B.R. for B^+ and B^0 to be 10%. For process (b) above, given equal numbers of D^{*0} and $D^{*\pm}$ in the debris of B decays one gets a D^+/D^0 ratio ≈ 2 . Using 20% and 2% for the respective B.R. yields a net rate of 8%. The total B.R. of $B \rightarrow \mu$ is thus 18%.

For charm production we take $\sigma = 20\mu\text{b}$ and an average semi-leptonic B.R. to muons of 10%.

For selection a, ($p_\mu > 6 \text{ GeV}/c$, $p_T > 0.6$) we have 1.5×10^4 events to examine and a yield of 19 B decays from process (a) and 5 from process (b), with a charm yield of 1300 events (650 pairs). The relevant muon acceptances are 60% for (a), and 20% for (b).

In addition to this straight forward cut on the prompt muon, which works well for muons from B decay, but loses 80% of the charm decays, we would select events where a muon is tagged as coming from a secondary vertex downstream of the primary interaction. To predict the success of this procedure we have computed the ratio $\delta z/\hat{z}$ for 5 D^\pm events found so far in E531. Here, δz is the estimated error in the z (beam direction) coordinate of each event, based on the actual momenta and angles of the observed decay tracks, and $\hat{z} = c\beta\gamma\tau$ is the expected decay length for a lifetime $\tau = 10 \times 10^{-13}$ sec. For these 5 events, having

respective D^\pm momenta of 9.8, 10.1, 16, 17, and 120 GeV/c, the corresponding ratios $\delta z/z$ are .22, .17, .14, .15, and .10, so that primary and secondary vertices are separated by 5 - 10 standard deviations. It should be noted that $\delta z/\hat{z}$ improves with D momentum because δz is dominated by multiple scattering in the emulsion for secondaries below ~ 8 GeV/c.

We estimate the efficiency of reconstructing three-prong secondary vertices (with a visible energy of greater than 10 GeV/c) could be as high as 80%. The background is primarily from nuclear interactions of pions.
 $= 8 \pi$'s/interaction \times (4% absorption length) \times (40%, $p > 10$ GeV) \times (70%, ≥ 3 prongs).
 We estimate the muon background to be $\leq 2 \times 10^{-3}$ from the secondaries.

For selection b, ($p_\mu > 3$ GeV/c, $p_T > 0.25$ for muon from secondary vertex), we have a yield of 960 charm decays and 5 B decays for 8×10^3 events examined. (This yield is corrected for double counting in selection a.)

To summarize, we have

	B Yield $B \rightarrow D^{*\mu\nu}$	B Yield $B \rightarrow D4\pi$ \downarrow $K^{*\mu\nu}$	Charm Yield	Background events to be scanned
Selection a $p_\mu > 6, p_T > 0.6$	19	5	1300	1.5×10^4
Selection b ($p_\mu > 3.5, p_T > 0.25$ secondary vertex)	--	5	960	8×10^3

E. Cost Estimates

Total
(in thousands)

Items in parentheses already exist.

1. Fermilab:

a. 20' x 30' of floor space, with provision for an upstream set of beam drift chambers. Utilities such as 30KW of 110 and 208V, water for magnet	-----
b. Up to 200KW of electrical power delivered for magnets	-----
c. 1 toroid, estimate 50 tons @ \$600/ton for cutting and machining, and \$5000 for the coils	\$ 35K
d. Extra muon steel (could be taken from existing E-531 iron) assume cost to be 100 tons @ \$300/ton	(\$ 30K)
e. Calorimeter steel (could be made from E-531 calorimeter by cutting only 3 of 16 existing 2" plates). Assume cost to be \$500/ton	(\$ 25K)
f. Small conventional magnet, estimated at \$1.00/lb for machined steel and \$3.00/lb for copper, with a 30% cost overrun included	30K
g. Prep electronics, mostly already in inventory	(\$ 90K)
h. Rigging, 16 days @ \$500/day	\$ 8K
i. 250 hours of computer time, @ \$400/hour	\$ 100K
j. Space in the village as provided for E531.	-----
k. Prototyping solid state detectors	\$ 50K

Existing Costs	(\$ 145K)
New Costs	\$ 223K

Total Costs	\$ 368K

2. Experimenters

a. Scintillation Counters

- i. Tubes, bases, power supplies, voltage dividers (\$ 100K)
- ii. Scintillation material (\$ 20K)
\$ 15K

Subtotal (\$ 120K)
\$ 15K

b. Solid state detectors

- i. Prototyping, (30K is already committed). (\$ 30K)
\$ 30K
- ii. Hardware (including cryostats and stands) for 33 detectors, @ 2K/detector \$ 66K
- iii. Electronics, 13000 wires @ \$25/wire \$ 325K

Subtotal (\$ 30K)
\$ 421K

c. Drift chambers

- i. 12 chambers @ \$2K/chamber (includes stands) \$ 24K
- ii. Existing multiple hit/wire readout system for 250 wires (\$ 25K)

Subtotal (\$ 25K)
\$ 24K

d. Gamma chambers

- i. Lead \$ 4K
- ii. Stand \$ 2K
- iii. Extruded tube chambers: 14 planes @ \$400/plane \$ 6K
- iv. Electronic readout of both ends of 1400 wires, @ \$6.00/channel \$ 17K

Subtotal \$ 29K

e. Calorimeter (exclusive of iron)		
i. Stand	\$	2K
ii. Hardware for 108 chambers, @ \$150/chamber	\$	16K
iii. Electronics - 864 lines read out both ends, @ \$6/channel	\$	10K
		<hr/>
	Subtotal	\$ 28K
f. Muon detector (exclusive of scintillator counters, toroid and range steel)		
i. Extruded tube drift chambers, 84 units @ \$100/unit	\$	8K
ii. Multiple hit/wire drift chamber readout system; 672 lines @ \$100/line (mostly existing)	(\$	59K)
	\$	8K
iii. Tube chamber hardware, 66 units @ \$100/unit	\$	7K
iv. Electronic readout of both ends of 792 wires, @ \$6/channel	\$	10K
		<hr/>
	Subtotal	(\$ 59K)
		\$ 33K
g. Emulsion related costs		
i. Precision front-end stand and emulsion movement mechanism	\$	50K
ii. Misc. hardware (for punching, etc.)	\$	50K
iii. Emulsion: 50 liters (@ \$7K/liter by the end of 1982, current cost is \$5K/liter)	\$	350K
iv. Pouring laboratory (being constructed for E531 at Fermilab)	(\$	80K)
v. Developing laboratory (exists at Ottawa)	(\$	100K)
vi. Developing costs (chemicals, etc. @ 10% of cost of emulsion)	\$	35K
vii. Emulsion scanning laboratories at Ottawa and in Japan	(\$	825K)
		<hr/>
	Subtotal	(\$1005K)
		\$ 485K

h. Computer (General Automation SPC 16/85)	(\$ 120K)
i. 1000 hours of AMDAHL 470 computer time at \$500/hour	\$ 500K
j. Misc. fast electronics	(\$ 30K) \$ 10K
k. Operating costs, 12 months @ \$5K/month	<u>\$ 60K</u>
Existing	(\$1389K)
New	<u>\$1605K</u>
Total*	\$2994K

*This total is within 30% of that estimated for the second run of E531. Based on experience gained in E531, we expect cost overruns to be less than 30%.

F. Time scale for the Experiment

We believe that with the good rate of progress on our existing E531 experiment, we have the capability of instituting a developmental program for solid state detectors. This program has already begun, with the placing of purchase orders for the prototype strip detectors from the Silicon Solid State Group at LBL. A testing cryostat is being designed and constructed by a student at Ohio State University. However, we believe this testing program will take two years and will require at least two prototypes before construction of the final detectors. It is important that such a program have clear goals generated by a pending experiment. Therefore, we propose the following schedule.

Summer, 1981	Complete testing of first prototypes.
Winter, 1982	Complete testing of final prototypes and commence full-scale construction.

Winter, 1983	Complete construction and commence installation.
Summer, 1983	Complete installation, have 1 month run to debug hardware.
Fall, 1983	Commence data run* of roughly 2-3 months.
Summer, 1984	First results of analysis appear.
Winter, 1986	Complete analysis.

*Note that emulsion data runs are necessarily short, well suited to the period of construction at Fermilab. Of course, the B-yield for the experiment would benefit a factor of 4 from pion beams available during Tevatron operation should it be available.

References

1. E531 preprints, N. Ushida, et al., "Measurement of the D^0 Lifetime," and "Measurement of the D^+ , F^+ , and Λ_c^+ Charmed Particle Lifetimes," manuscript in preparation (1980).
2. M. Kobayashi and K. Maskawa, Prog. Theor. Phys. 49 652 (1973).
3. See, e.g., John Ellis, "Status of Gauge Theories," CERN preprint Th-2701 (1979); J. A. Harvey, P. Ramond, and D. B. Reiss, "CP Violation and Mass Relations in $SO(10)$," Cal Tech preprint 68-758 (1979); S. Nandi and K. Tanaka, Ohio State University preprint C00-1545-270 (to appear in Phys. Lett. B, May 1980).
4. J. E. Lamport, et al., Nucl. Instr. and Meth. 134 71 (1976).
5. V. Radeka and R. A. Boie, Proceedings of 1979 Nuclear Science Symposium (to be published in IEEE Trans. Nuc. Sci.).
6. We wish to thank Stan Snowdon of Fermilab for aiding in magnet design and computing typical field profiles for this magnet.
7. S. L. Stone, et al., Nucl. Instr. and Meth. 151 387 (1978).
8. A. Babaev, et al., Nucl. Instr. and Meth. 160 427 (1979).
9. Cross sections are plotted for data as close to 375 GeV/c as possible. The ϕ point is at 150 GeV/c from K. J. Anderson, et al., Phys. Rev. Lett. 37, 799 (1976). The ψ comes from a fit of the form $\sigma = 350 e^{-9\sqrt{\tau}}$, where $\tau = m/\sqrt{s}$, to existing data listed in the review talk by J. Pilcher, Proc. Int. Symposium on Lepton and Photon Interactions, 185 (1979). The T point is also an extrapolation to 375 GeV from the data presented by W. Kienzle, op. cit., 161 (1979). The kaon point, quoted as 4 times the K_S^0 cross section, is from N. W. Biswas, preprint "Inclusive Production of π^0 , K_S^0 , Λ^0 , and $\bar{\Lambda}_0$ in 100, 200 and 360 GeV/c π^-p Interactions," Fermilab No. 37870 (1980) and Notre Dame preprint 80-0068. The charm cross section is from J. Sandweiss, et al., Phys. Rev. Lett 44 1104 (1980).

10. B. L. Combridge, Nucl. Phys. B151 429 (1979); H. Fritzsch, Phys. Lett. 86B 164 (1979).

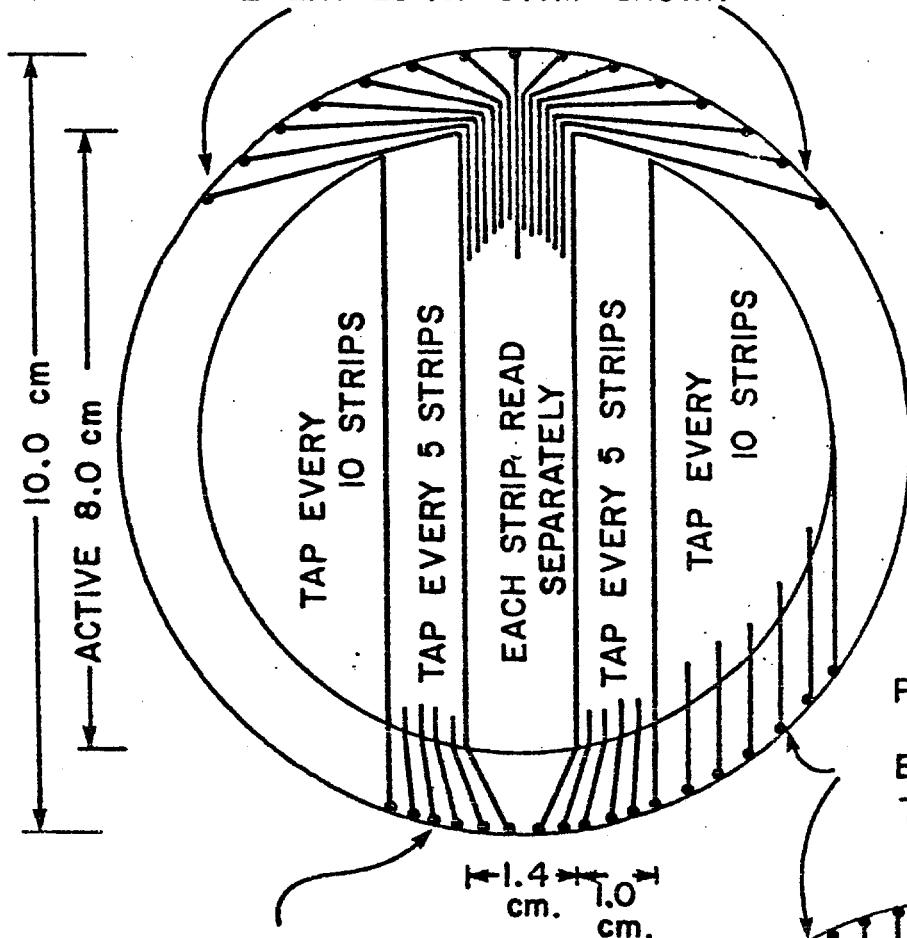
Figure Captions

1. Layout of position-sensitive silicon detectors. (a) Beam detector wafer; (b) Vertex detector wafer; (c) Downstream detector wafer.
2. Elevation view of the hadron hybrid spectrometer.
3. Emulsion module and movable mounting stage.
4. (a) Integral distribution in laboratory production angle θ for charged hadrons and converted electrons from 360 GeV/c π^-p events.
(b) Fraction of tracks masked in the x projection vs. θ for various resolutions in projected slope $\Delta x'$, for the above events.
5. Pole-piece geometry and calculated magnetic field for the spectrometer magnet shown in Figure 2.
6. Charged particle momentum resolution for tracks passing through the downstream drift chamber (solid curve) and through the downstream silicon detectors (dashed and dotted curves).
7. Neutral hadron detection efficiency. Fraction of hadron showers separated by more than 5cm in the x projection vs. production angle θ (solid curve); angular distribution of K^0 from $B \rightarrow \psi K^0 \pi$ decay (dotted curve).
8. Momentum distributions of muons from π decay in ordinary hadronic events (dotted curve), from $B \rightarrow D \rightarrow \mu$ cascades (dashed curve), and from $B \rightarrow D^* \mu \nu$ (solid curve).
9. Transverse momentum distributions for muon from the three sources listed above.
10. Experimental cross sections for ϕ , ψ , and T production, and for K and D production from pions of ~ 350 GeV.

POSITION-SENSITIVE SILICON DETECTOR
(ACTUAL SIZE)

b. VERTEX DETECTOR WAFER

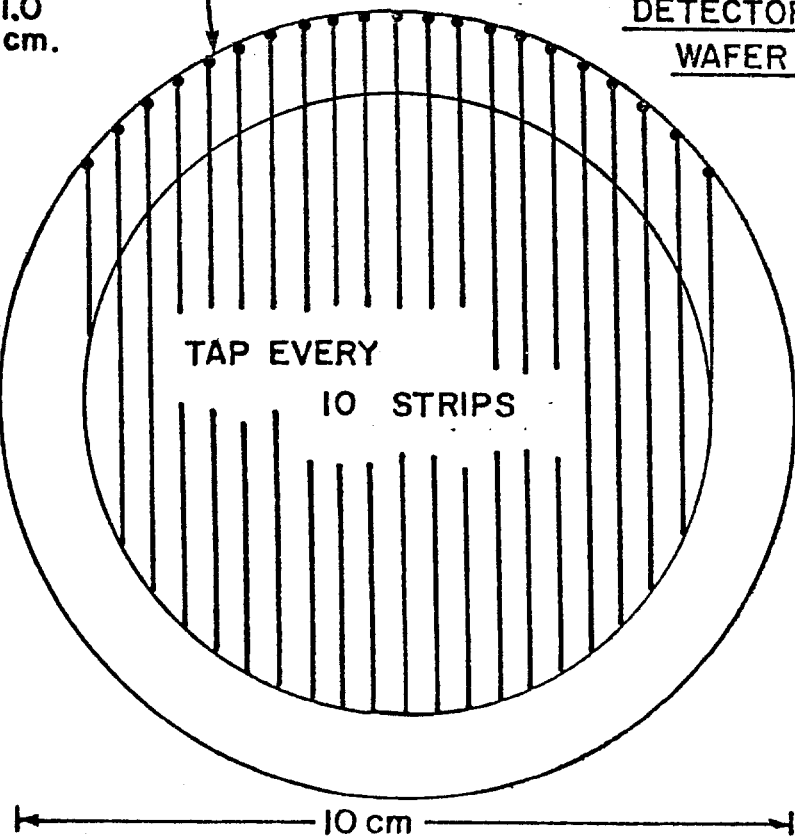
PAD SPACING 0.25 mm.
EVERY 25 TH STRIP SHOWN



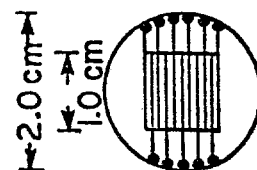
PAD SPACING 0.3 mm.
EVERY 10TH TAP SHOWN

c. DOWNSTREAM DETECTOR WAFER

ACTIVE 8.0cm



a. BEAM DETECTOR WAFER



TAP EVERY 5 STRIPS

PAD SPACING 0.4mm.
EVERY 5TH TAP SHOWN

NOTE . ALL WAFERS 0.4mm. THICK
ALL STRIPS 10 μ WIDE
40 μ CENTER-TO-CENTER

PAD SPACING 0.5 mm.
EVERY 10TH TAP SHOWN

c. DOWNSTREAM DETECTOR WAFER

Figure 1

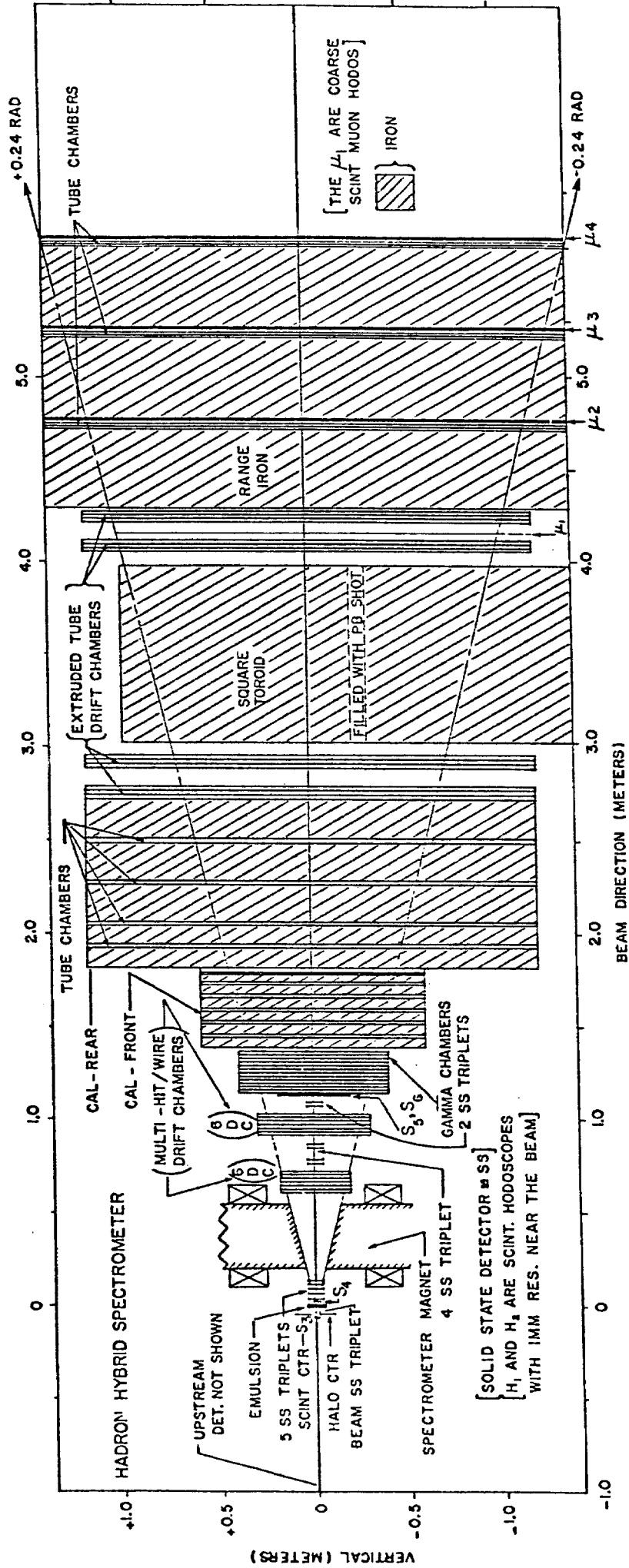
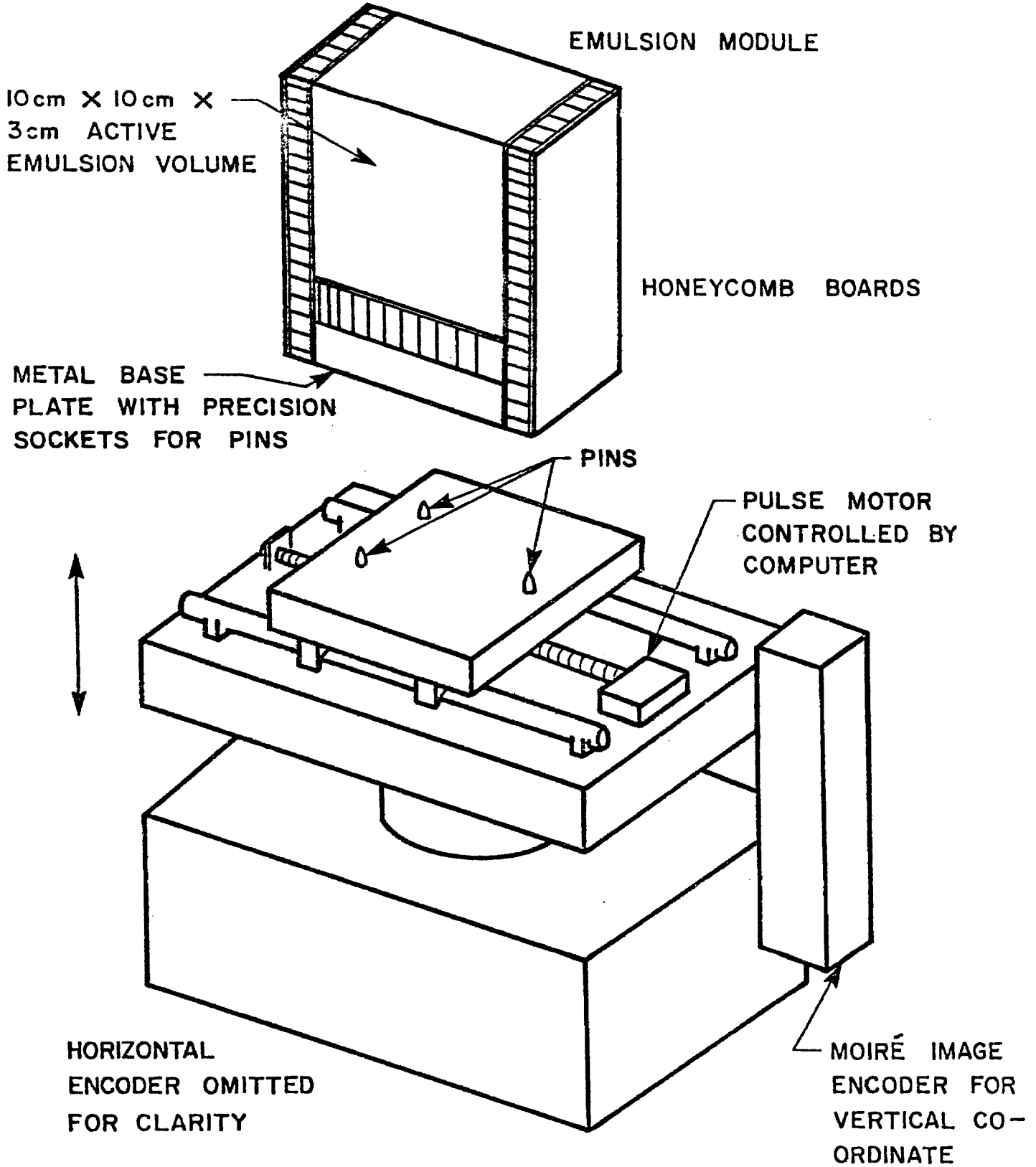


Figure 2



SCHEMATIC DRAWING OF EMULSION STAND

Figure 3

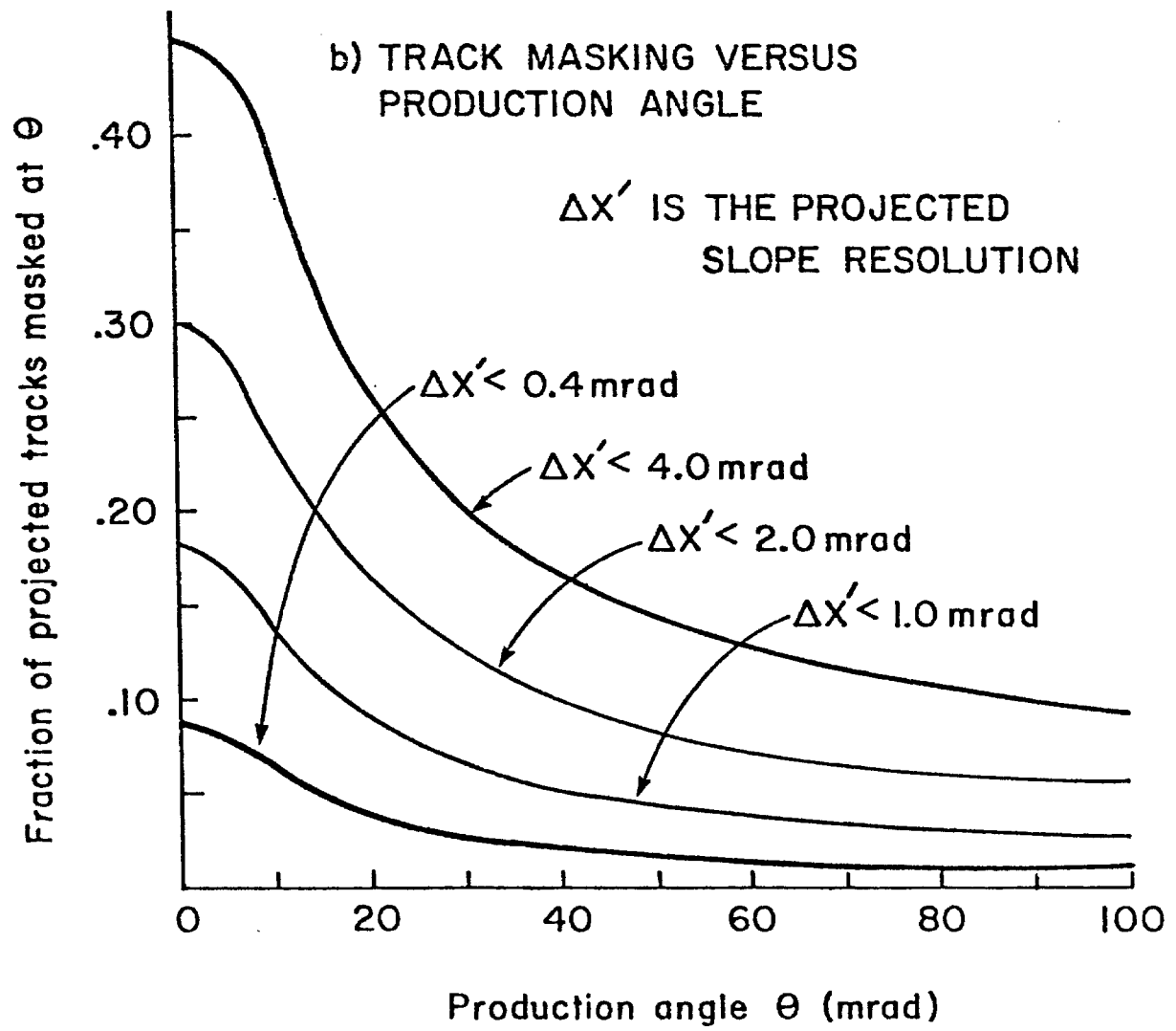
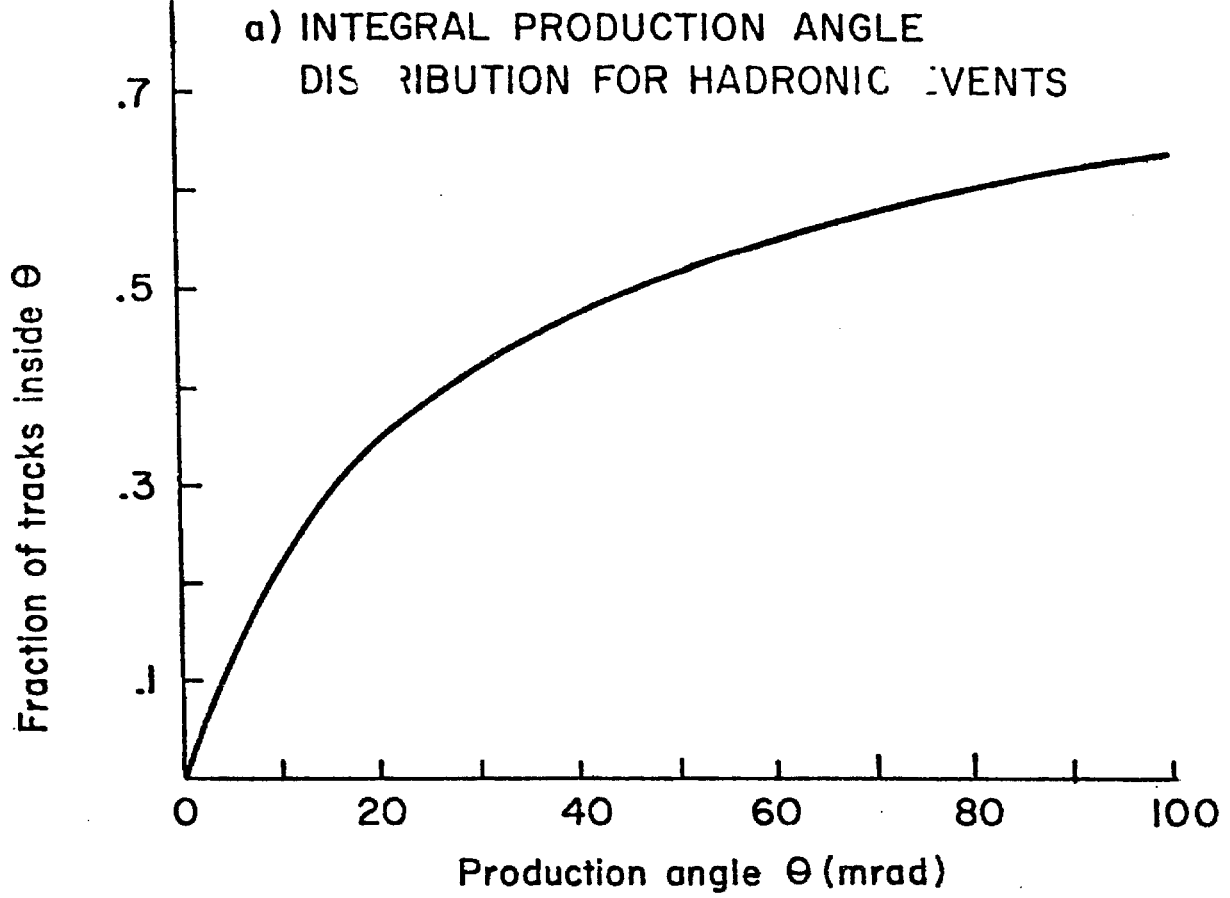


Figure 4

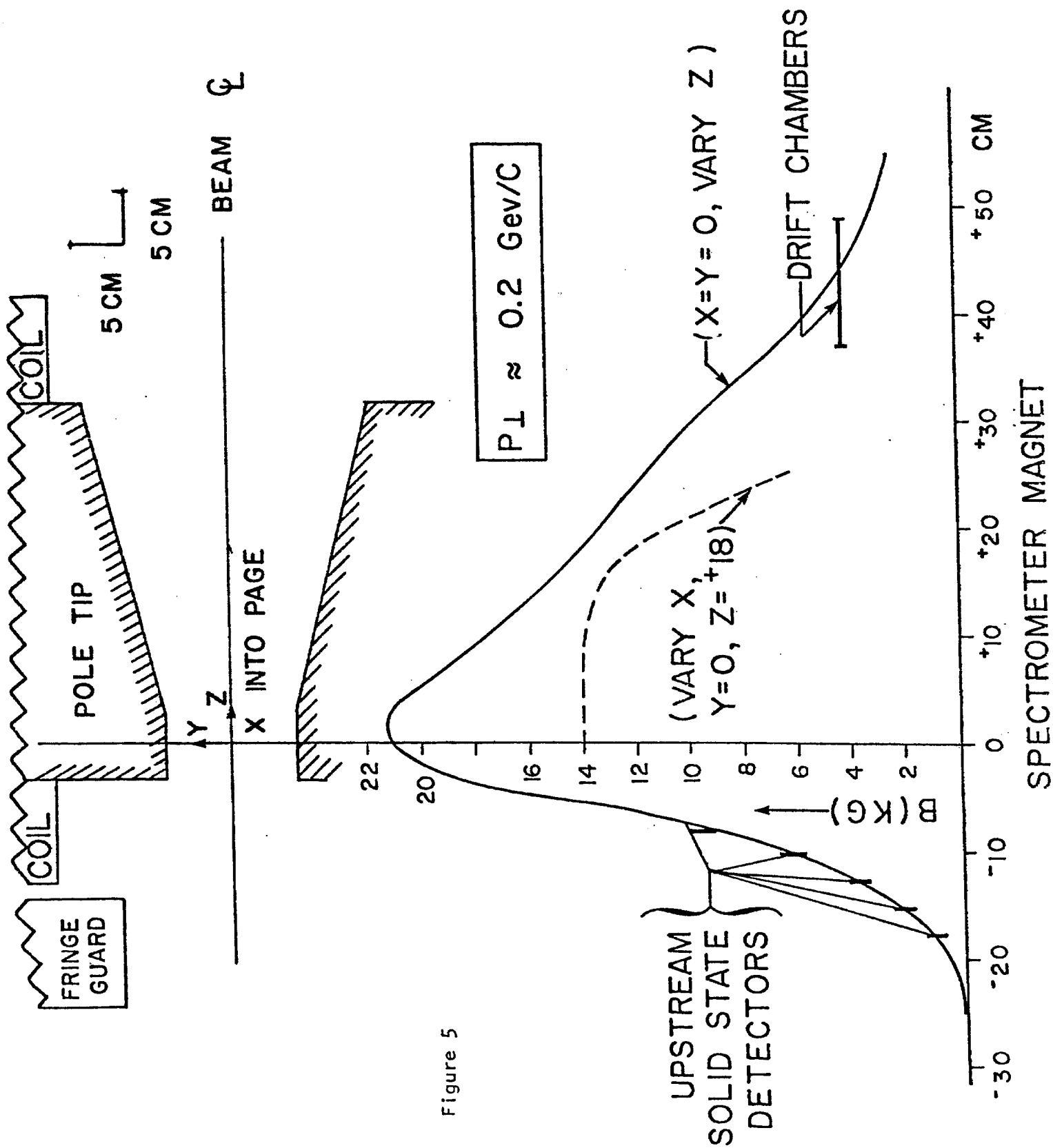


Figure 5

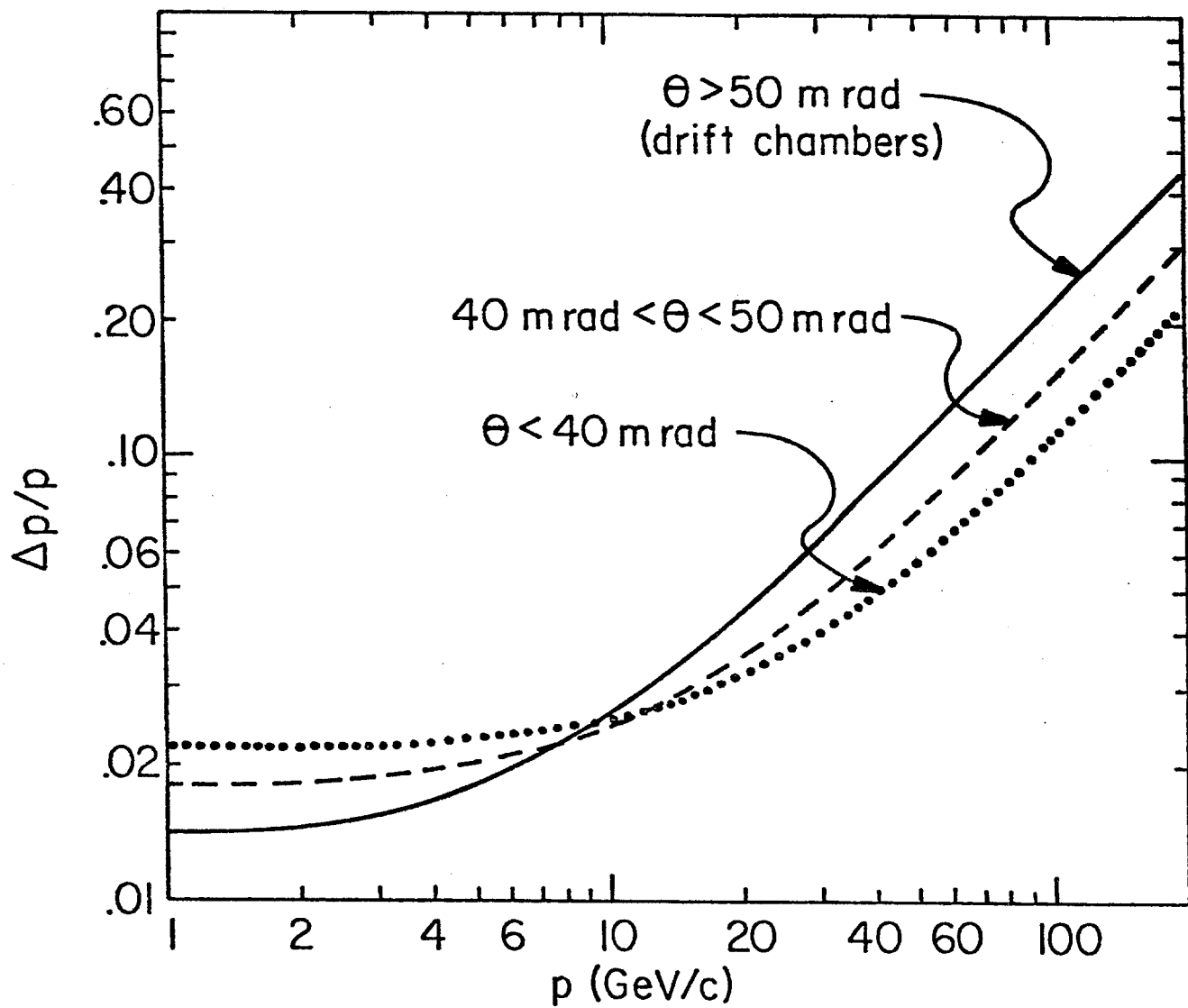


Figure 6

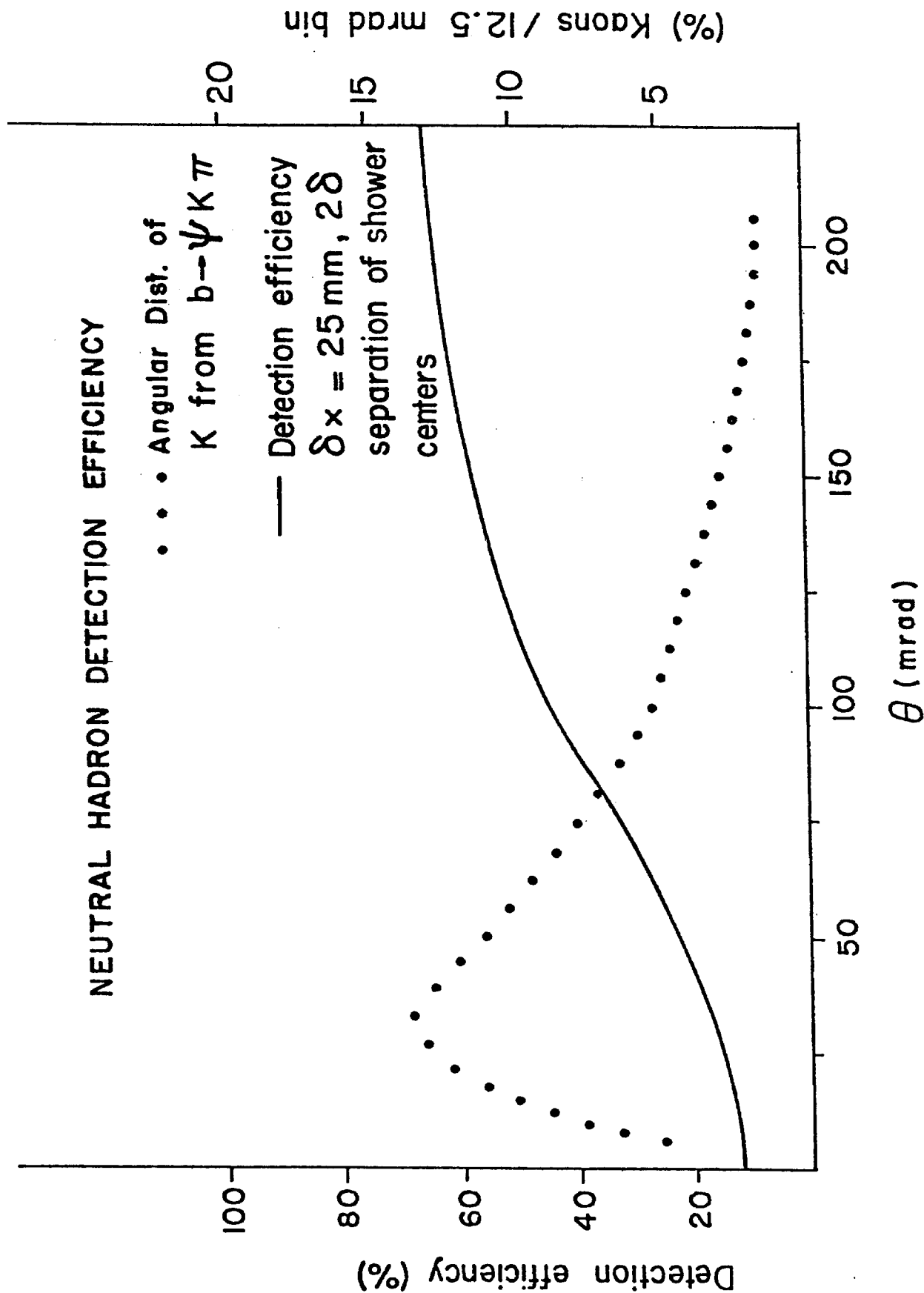
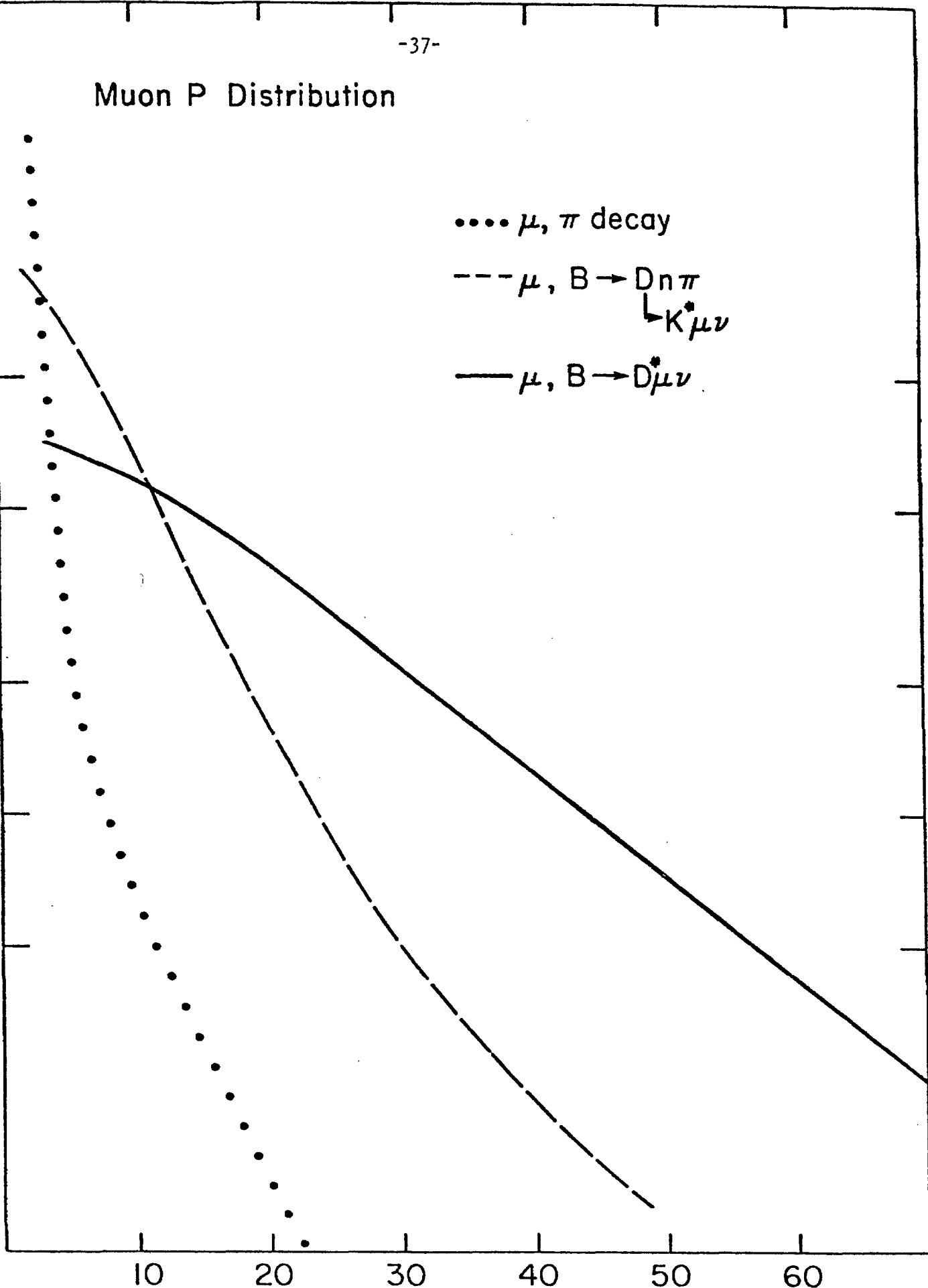


Figure 7

Muon P Distribution

Events / 5 GeV (Arbitrary Scale)

- μ, π decay
- $\mu, B \rightarrow D n \pi$
 \swarrow
 $K^* \mu \nu$
- $\mu, B \rightarrow D^* \mu \nu$



P GeV/c
Figure 8

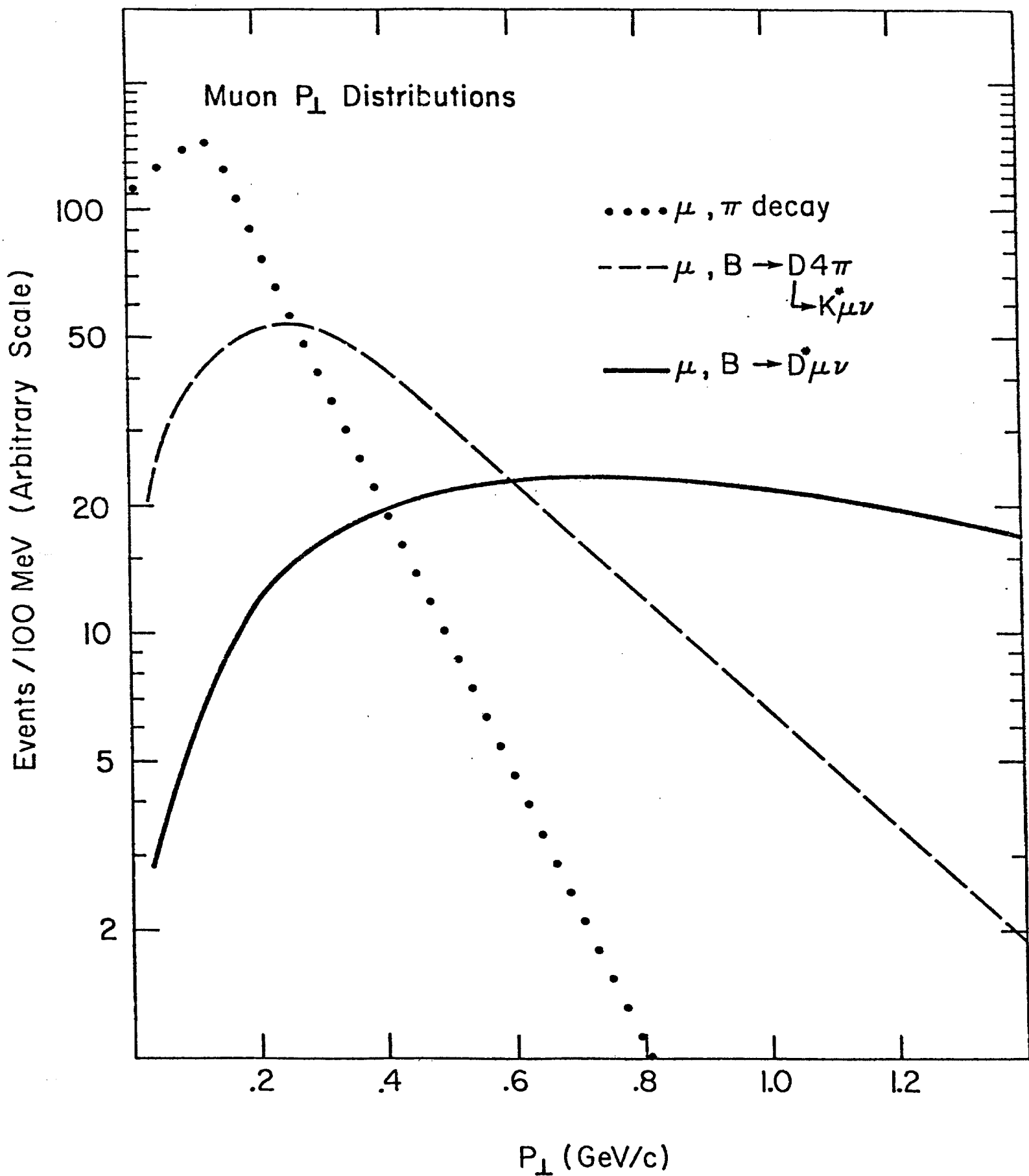


Figure 9

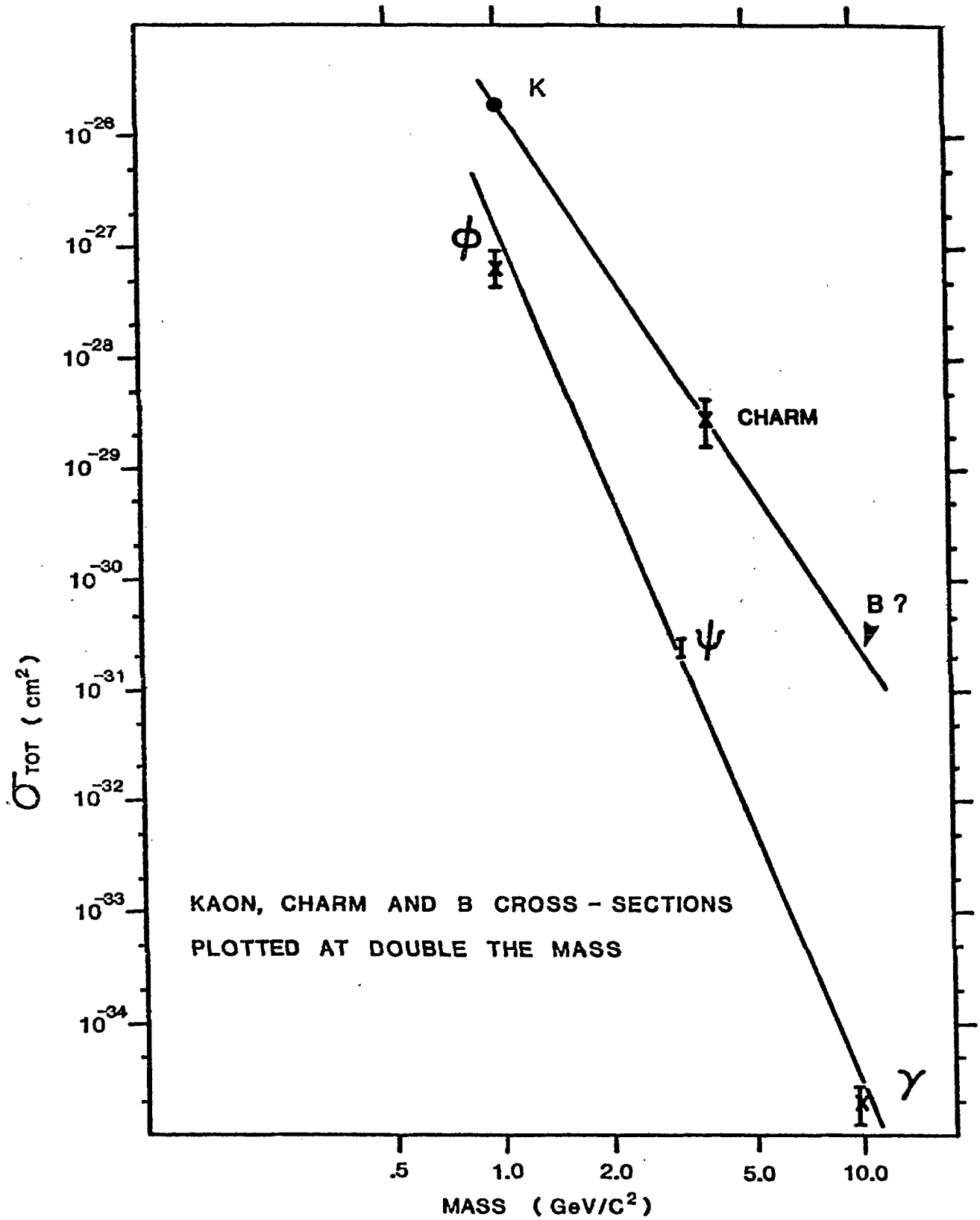


Figure 10

Appendix I

Prototyping of Position-Sensitive Semiconductor Detectors

Though developing solid state detectors will require an extended program, we believe it may be informative to delineate our first steps.

The semiconductor group of the research services division of Lawrence Berkeley Laboratory has agreed to construct six prototype devices according to the specifications shown in Figure I-1 (page 43). These prototypes are designed to test both of the readout techniques to be used in this experiment. Each is made from a wafer of high-resistivity P-type silicon 2cm in diameter and 0.4mm thick. The central active area, 1cm x 1cm square, is given an N-type layer on one side by a standard phosphorous diffusion technique, and the inactive outer portion is covered with an oxide layer. On the other side of the wafer, a pattern of 250 gold strips 0.01mm wide with 0.04mm center-to-center spacing will be laid down over a similar pattern of P-type boron implants covering this active area. These gold strips are fanned out over the inactive region so that at the rim the connection pads have a spacing of 0.25mm. Each detector will then be mounted on a ceramic ring holder to which external connections can be attached. Since every strip is brought out, these prototypes may be used to test both the individual-strip and the charge-division readout techniques with complete flexibility to choose the number of strips between taps.

In order for the charge-interpolation method to succeed it is important to stabilize the impedance between strips. This will be done by protecting the layer between strips with an oxide layer. At present, neither how well the surface under the oxide "pinches off", (i.e., how the impedance between strips varies with applied voltage), nor what noise levels and impedance values can be achieved is known. A preliminary series of tests will therefore be performed on some laboratory samples with 0.5mm spacing which are easier

to produce. If these tests are satisfactory, the six prototypes will then be constructed according to plan.

Ohio State University has committed \$7K to this first stage of testing, which should take 2-3 months, and another \$18K to the building of the six prototypes, which will take approximately six months more. Because detector noise may be a problem, Ohio State is constructing a cryostat with an internal heating system which will permit controlled stabilization of devices between ambient and liquid nitrogen temperatures.

Even in the initial test setup we must be prepared to detect (with good pulse-height accuracy) signals of a few femtocoulombs from over 100 lines. Thus, the detecting electronics and the test setup must be quite sophisticated. Initially, we propose to borrow about 100 channels of the liquid argon ADC systems designed by Tom Droege. This is one full CAMAC crate and will cover about 4mm of the first prototype. These have a one femtocoulomb least count and a four thousand count dynamic range. Since they are CAMAC modules, it will be easy to connect them to a small computer. This setup should allow understanding many of the properties of the detector such as charge collection efficiency and charge collection time. To make solid state detectors truly effective, we must have even lower noise amplifiers (0.2 femtocoulombs random noise), and 5% pulse height capability for more than ten thousand lines. Developing these amplifiers and a low cost CCD parallel in-series out analogue storage system with fast ADC conversion presents an electronic engineering task which must be pursued simultaneously with hardware development.

Of course, the bottom lines are detection efficiency, single-track spatial resolution and multitrack separation capability. Since these detectors will have state-of-the-art capability, many tests will have to be performed with a stack of at least three identical detectors in a high-momentum test beam.

Though for our proposed usage radiation damage will not be a problem, such may not always be the case for all applications. If solid state devices were to be used as vertex detectors in a colliding beam apparatus, radiation during injection could be severe. Therefore, we will also study the effect of radiation damage for our prototype devices.

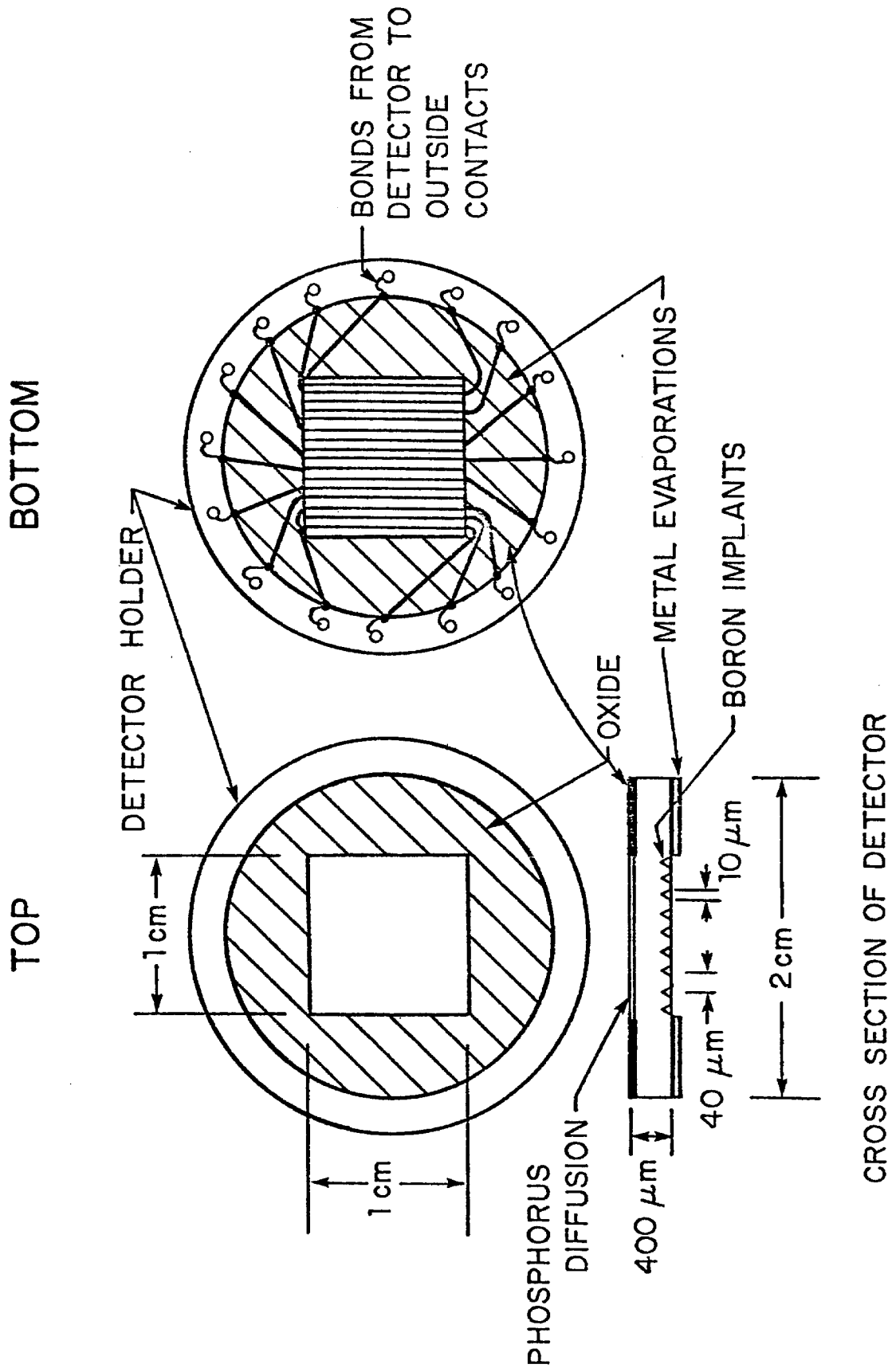


Figure 1-1

Appendix II

Event Reconstruction

This appendix is still in preparation, but will be available within two weeks.